AIP | Review of Scientific Instruments

Steady-state photoluminescent excitation characterization of semiconductor carrier recombination

J. S. Bhosale, J. E. Moore, X. Wang, P. Bermel, and M. S. Lundstrom

Citation: Review of Scientific Instruments **87**, 013104 (2016); doi: 10.1063/1.4939047
View online: http://dx.doi.org/10.1063/1.4939047
View Table of Contents: http://scitation.aip.org/content/aip/journal/rsi/87/1?ver=pdfcov
Published by the AIP Publishing

REVIEW OF SCIENTIFIC INSTRUMENTS **87**, 013104 (2016)

Steady-state photoluminescent excitation characterization of semiconductor carrier recombination

J. S. Bhosale,[1,2,a] J. E. Moore,[2] X. Wang,[2] P. Bermel,[2] and M. S. Lundstrom[2]
[1]*Intel Corporation, Hillsboro, Oregon 97124, USA*
[2]*Department of Electrical and Computer Engineering, Purdue University, West Lafayette, Indiana 47907, USA*

(Received 24 June 2015; accepted 13 December 2015; published online 14 January 2016)

Photoluminescence excitation spectroscopy is a contactless characterization technique that can provide valuable information about the surface and bulk recombination parameters of a semiconductor device, distinct from other sorts of photoluminescent measurements. For this technique, a temperature-tuned light emitting diode (LED) has several advantages over other light sources. The large radiation density offered by LEDs from near-infrared to ultraviolet region at a low cost enables efficient and fast photoluminescence measurements. A simple and inexpensive LED-based setup facilitates measurement of surface recombination velocity and bulk Shockley-Read-Hall lifetime, which are key parameters to assess device performance. Under the right conditions, this technique can also provide a contactless way to measure the external quantum efficiency of a solar cell. © *2016 AIP Publishing LLC.* [http://dx.doi.org/10.1063/1.4939047]

I. INTRODUCTION

A wide variety of characterization techniques involving the photoluminescence (PL) of semiconductors offer crucial insights into various material properties. Examples of these properties include defect states,[1] Shockley-Read-Hall (SRH) lifetimes,[2] and surface recombination velocities (SRVs),[3] which has significant importance for opto-electronic devices like solar cells. The contactless and nondestructive nature of these techniques is suitable for in-line monitoring of device quality during fabrication. For the characterization of these devices, photoluminescent excitation (PLE)[4] spectroscopy is a yet another PL technique, however, it has not been a prevalent technique compared to the techniques such as time-resolved PL[5] or PL spectral measurements.[6]

In PLE spectroscopy, monochromatic light with photon energy larger than the semiconductor bandgap energy excites excess electrons and holes. As these carriers radiatively recombine, the resulting PL signal is recorded as a function of excitation wavelength. The PLE spectrum is then defined as[7]

$$PLE(\lambda_{in}) = \frac{\phi_{emit}}{\phi_{in}(\lambda_{in})}, \quad (1)$$

where, ϕ_{in} is the incident photon flux at wavelength λ_{in}, and ϕ_{emit} is the PL emission flux from the sample. In an experiment, if ϕ_{in} is maintained as a constant at all wavelengths, then the PLE becomes proportional to PL emission flux, and the PLE curve is obtained by sweeping the incident light wavelength over a desired spectral region.

The strength of the PL emission is affected by bulk and surface recombination. The relative importance of these two contributions depends on the excitation wavelength, which allows determination of SRV and SRH lifetime with PLE measurements, as illustrated below. Therefore, these measurements can be used to compare the device quality with respect to an appropriate standard. In contrast with the time resolved photoluminescence (TRPL) technique, the PLE technique does not yield bulk lifetime information directly. However, when coupled with an appropriate simulation flexible enough to model both experimental PLE and TRPL data, both sets of data can be combined to obtain a superior accuracy in lifetime and surface recombination velocity measurements, compared to that obtained with individual techniques.[8]

In addition to measuring bulk lifetime and surface recombination velocity, the direct correlation of PLE with the open circuit voltage (V_{OC}) of a solar cell[9,10] makes PLE a contactless method to evaluate the performance of a solar cell. For high quality crystalline solar cells, PLE has been shown to be equivalent to the external quantum efficiency (EQE),[11] which is an important indicator of solar cell performance.

State-of-the art semiconductor device fabrication is a complex process, involving new materials and continually changing processes, in which research projects aim to improve efficiency and fabrication costs. Therefore, many devices are routinely fabricated and characterized in a lab or a foundry. PLE being a contactless characterization technique, presents a great advantage in filtering out defective devices at an early stage of the process. Hence, in order to develop PLE as an in-line characterization technique requires a fast, sensitive, and cost effective instrumentation to observe a trend where a coarse resolution is sufficient.

Traditionally, a broadband source such as a halogen lamp coupled to a monochromator is used for PLE excitation.[12] In this case, the excitation light can be weak, particularly in the visible to ultraviolet region,[13] which requires a sensitive detector such as a photomultiplier tube (PMT) to detect the PL signal. However, a wide variety of semiconductors have band gaps in the infrared (IR) region, requiring costly infrared PMTs. This fact has greatly impeded the adoption of PLE as a cost-effective in-line characterization technique. Although laser-based sources such as a broadband tunable laser (e.g.,

[a]This research was performed while J. Bhosale was at Purdue University, West Lafayette, Indiana 47907, USA.

Titanium:sapphire) or a supercontinuum source covering the full spectrum would seem to be an ideal PLE source, because of their high brightness and beam quality,[14] they require expensive pump lasers and generally have limited spectral tunability. Fortunately, these limitations can be overcome with an array of bright light emitting diodes (LEDs) spanning a broad wavelength range, which represent a compromise between broadband sources and narrowband laser emitters. When used as a means of detecting recombination, PLE measurements do not need the extremely high resolution required for other applications, such as resolving excited states, so for this particular application the LED setup is faster and more efficient than traditional methods.

In recent years LEDs have emerged as efficient bright light sources with excellent spatial and temporal stability. With anticipated increases in brightness and efficiency[15] along with their small size and narrow spectral bands, they can provide nearly comparable performance for optical spectroscopy. As a fortunate side effect of increasing manufacturing scale, LEDs also now offer a significant cost-effective improvement over conventional sources for PLE. Bright LEDs are already commercially available covering the spectral region from 300 nm to 1000 nm, with successive spectral intensity peaks as close as 10 nm.[16] With additional temperature tuning of suitable LEDs, higher resolution can be obtained in the PLE spectra. In this article, a method for measuring PLE spectrum with LED sources is described, and its performance is evaluated on solar-cell materials. The design produces a low cost PLE setup that is suitable for fast in-line characterization.

II. CONSTRUCTION

A. Analytical framework

In order to choose the appropriate range of wavelengths and detectors needed for our experiment, it is helpful to first create a simple analytical framework to understand and predict the expected PLE signal. This framework is intended to address the ideal case of a device without effects such as non-radiative recombination or band bending, which are usually present in real samples. Thus, when analyzing actual devices, we recommend using a numerical modeling approach, as we will demonstrate in Section III. Consider an illuminated sample following Beer's law with absorption coefficient α. The absorbed photons generate excess charge carriers Δn, which diffuse with diffusion constant D and re-emit as photons at the bandgap energy with a radiative lifetime τ_b,

$$0 = D\frac{d^2\Delta n(x)}{dx^2} - \frac{\Delta n(x)}{\tau_b} + \alpha I_0 e^{-\alpha x}. \quad (2)$$

Assuming all excess carriers recombine at the surface ($x = 0$), this yields a steady state equilibrium population,

$$\Delta n(x) = \frac{\alpha I_0 \tau_b}{1-\alpha^2 D\tau_b}\left(-\frac{S+D\alpha}{S+\sqrt{\frac{D}{\tau_b}}}e^{-\frac{x}{\sqrt{D\tau_b}}} + e^{-\alpha x}\right), \quad (3)$$

where S is the surface recombination velocity and τ_b is the bulk lifetime. Under low injection conditions, where recombination events are limited by the minority carrier concentration, the total steady-state recombination and PLE signal are both proportional to the carrier density. Thus, the PLE signal is given by

$$PLE(\lambda_{in}) = B_{rad}N_A\frac{\alpha I_0\tau_b}{1-\alpha^2 D\tau_b}\left(-\frac{S+D\alpha}{S+\sqrt{\frac{D}{\tau_b}}}\sqrt{D\tau_b} + \frac{1}{\alpha}\right). \quad (4)$$

We can plot the PLE signal as a function of surface recombination velocity and absorption rate as shown in Fig. 1. It is evident that the greatest sensitivity to surface recombination can be seen for absorption coefficients α just above 10^5 cm^{-1}. For direct bandgap materials suitable for solar cells, such values often occur above the bandgap energy.[17]

We note that this model is somewhat simplified, in that it assumes a semi-infinitely thick wafer with only band-to-band recombination in the bulk. As a result, we see unrealistically high simulated PLE close to 1 for small absorption coefficients. In an actual device, this region would correspond to long wavelength photons with energies too small for efficient absorption. Realistically the PLE signal would be much smaller, as these photons would be lost through transmission, or else the generated carriers would recombine non-radiatively. A more complete analytic model or numerical simulation using photon recycling is needed to capture these effects.[8]

B. Instrumentation challenges

The intense and narrow band radiation offered by LEDs has already been exploited by various types of spectroscopy techniques.[18,19] However, their use in sensitive PL spectroscopy, in which signals can become quite small, requires additional instrumentation for a reliable detection—particularly since an LED source usually produces weak broadband emission, which can overlap with the infrared PL spectrum. This radiation can be attributed to the weak absorption coefficient below the band gap energy of a non-thermal emitter that may exist due to the deep level impurities.[20,21]

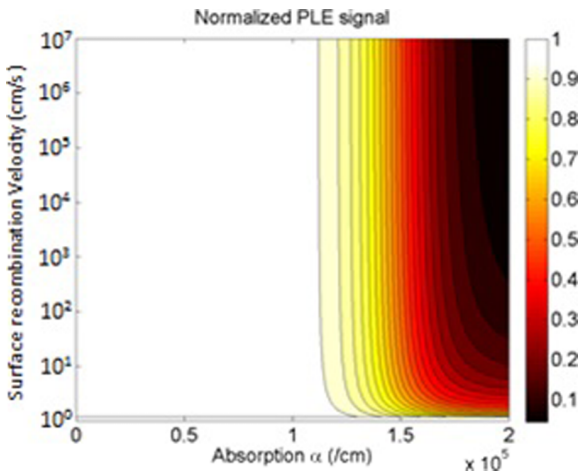

FIG. 1. Normalized PLE signal, as a function of the absorption and the surface recombination parameters.

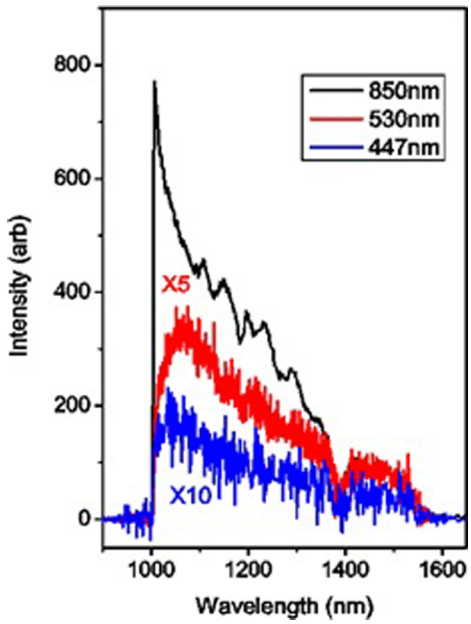

FIG. 2. Transmission spectra of the 1000 nm long-pass filter indicating LED leak. The spectra were obtained with LEDs with peak wavelength at 850 nm, 530 nm, and 447 nm.

Therefore, in a typical PL setup, IR radiation from the LED scattered by the sample may enter the long-pass optical filter used to prevent the incident light from reaching the detector, causing a significant error in the PL measurement. Figure 2 shows the spectra of IR radiation leaking through a 1000 nm long-pass filter for LEDs with different peak wavelengths. The spectra indicate that the intensity of leaking IR radiation significantly decreases as the difference between the filter cutoff and peak wavelength of the LED increases. However, in practice, even the LEDs with peak wavelengths significantly away from the filter cutoff can saturate the detector signal when observing extremely weak PL signals, such as those generated by thin films.

A further investigation of this issue reveals that even the laser diodes used in TRPL measurements are not immune to this leakage and can surprisingly lead to highly erroneous lifetime values. In order to demonstrate this effect, a modular Horiba TCSPC system was used as shown in Fig. 3(a). In this system, a beam from 635 nm pulsed laser diode was incident on a GaAs bare wafer sample. The angle of incidence was set in such a way to avoid any specular reflection of the laser from entering the PMT collection path. In addition, an 850 nm long-pass filter inside PMT rejects any scattered laser light from the sample or the sample chamber walls. Figure 3(b) shows the comparison of TRPL measurements obtained with and without Schott KG-3 heat absorbing glass,[22] used to prevent the IR leak from the laser diode. The curves clearly indicate that the IR leak completely overwhelms the detector, so that the lifetime information from the GaAs sample is effectively lost.

In the case of PLE measurements, different LEDs are used to cover a wide spectral range. A suitable LED array should cover the absorption spectrum of the samples being tested, with enough distinct wavelengths to give the required spectral resolution. Details on the LEDs used are provided in the Appendix. Since the IR leakage of the LED in Fig. 3 completely overwhelms than that of the GaAs PL, an entrance grating is a needed to shape the spectral bandwidth of the incident radiation, effectively preventing the IR leak. The details of the experimental setup are presented in Sec. II C.

C. Experimental setup

The experimental setup shown in Fig. 4 mainly consists of a LED source, two monochromators, and transfer optics. A temperature controlled LED matrix is used as a light source to provide excitation at different wavelengths. The LEDs in the source are arranged in a 4×4 grid on an X-Y-Z stage to provide excitation wavelengths ranging from 1000 nm to 350 nm in approximately 50 nm steps. A selector box is used to switch between LEDs, and the X-Y-Z stage is adjusted to align the LED in use with the collimation lenses of the first monochromator. Further details such as the emission spectra of the LEDs can be found in the Appendix. In order to optimize the light throughput over the entire spectral range, achromatic optical lenses with appropriate focal lengths and antireflection coating were used. Optical mirrors can be used instead of lenses, if better performance is required in a specific spectral region. The light from the source is collected and focused on an entrance slit of the first monochromator. The exiting light is then collimated and directed towards an optical grating

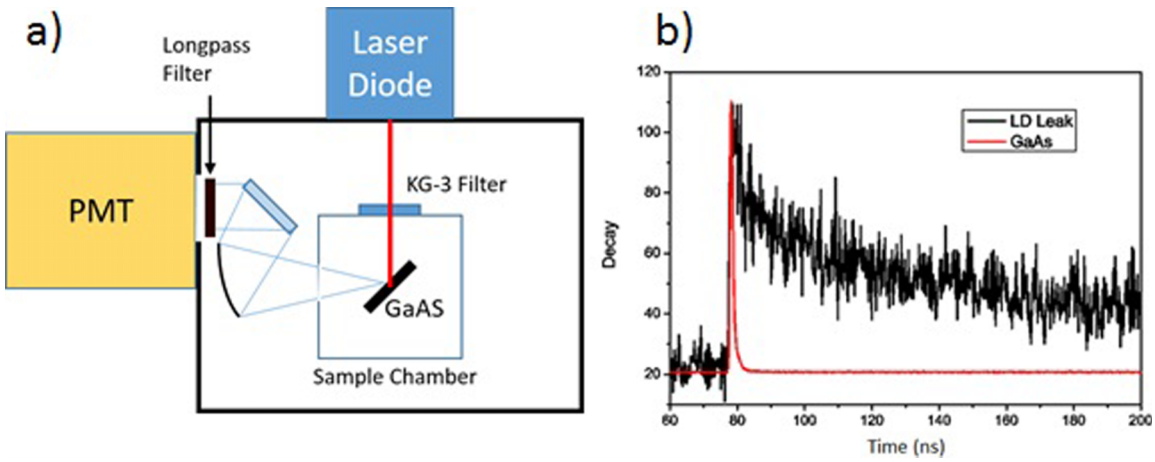

FIG. 3. (a) Horiba TCSPC system (b) TRPL decay comparison of a GaAs wafer with and without the leakage observed from a 635 nm laser diode.

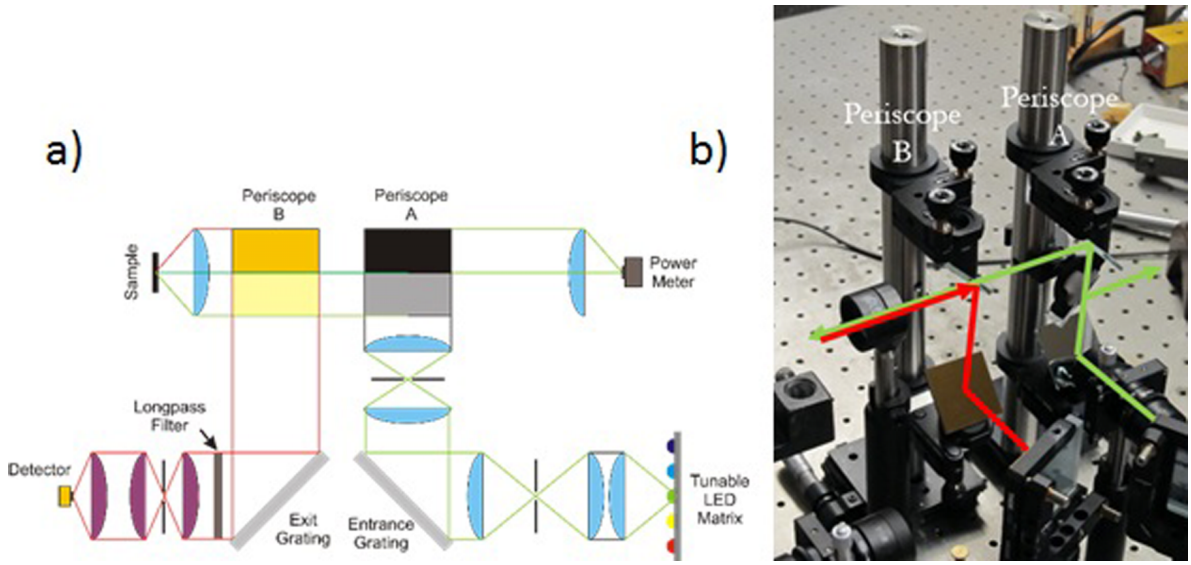

FIG. 4. LED based PLE setup: (a) schematic; (b) periscope assembly, with incident and PL beam paths highlighted.

with 600 lines/mm groove density and 500 nm blaze angle. The diffracted beam is then focused on the exit slit of the monochromator. The PL from the grating is then detected by a Si detector with a high gain ($\sim 2 \times 10^8$) amplifier connected to a lock-in amplifier, which also controls the LED intensity modulation. The angle between the incident and diffraction beams is also set at 90° and the grating angle is set constant in order to observe the PL radiation while rejecting any scattered incident radiation. A long-pass optical filter with appropriate cutoff is used to further eliminate the radiation that may arise due to higher order diffraction or scattering from grating imperfections.

For alignment convenience, the angle between incident and diffracted beams is set at 90°. The light exiting from the first monochromator is then collimated in order to split it into two parts of equal intensity for power measurement and sample exposure. However, due to the asymmetric spectral intensity around the peak wavelength of a LED[20] as shown in Fig. 5, the beam contains asymmetric intensity distribution perpendicular to the grating axis. Therefore, the periscope A assembly shown in Fig. 4(b) is used to rotate the collimated beam by 90° to ensure that the intensity measured is independent of the spectral asymmetry mentioned above. In addition, the periscope design ensures that two beams go through an equal number of mirror reflections.

An excitation spot size of 100 μm (or a different size) can be achieved by adjusting the slit width of the first monochromator. The PL radiation emitted from the sample upon excitation is collimated by the same lens; half of this beam is reflected down the periscope B to restore the original image orientation by a 90° rotation. The beam then enters the second monochromator on a grating with 600 lines/mm groove density and blaze angle optimized for 1 μm.

For in-line applications where a fast measurement is required, the LEDs could be arranged in an alternative configuration. Here, the LEDs would be placed at different precise incident angles of the grating to achieve the same angle of diffraction, without the need to move the grating mechanically. The excitation wavelength could instead be changed by simply switching on the desired LED.

III. EXPERIMENTS

For maximally stable spectral output, a LED must be operated at a constant temperature. Although the peak emis-

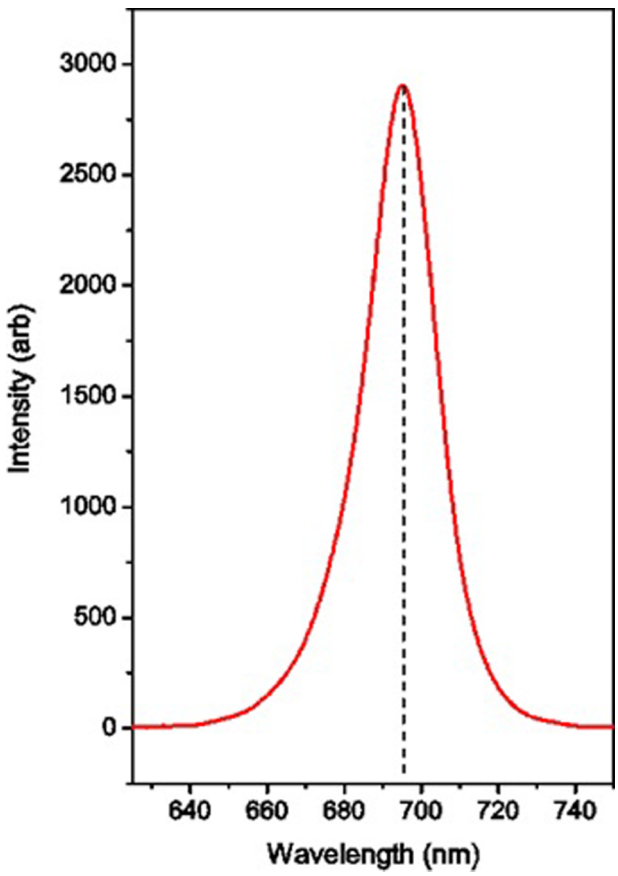

FIG. 5. Intensity spectrum of a red LED, showing the asymmetry about the peak wavelength.

sion intensity of a LED improves with decreasing temperatures,[23] the LED source was kept at 20 °C for all experiments to avoid moisture condensation. The grating angle of the first monochromator is set at the peak intensity wavelength of the chosen LED. The bandwidth of the excitation was chosen in the range of 2 nm–5 nm and kept unchanged throughout the experiment. A constant photon flux is achieved for each individual color LED by adjusting its current to match prior measurements from the photodetector. Once the sample is excited with the current LED, the second monochromator grating is rotated to scan for the PL signal, and it is set where the PL signal maximum occurs. The second monochromator slit width is then adjusted to optimize the PL signal.

In order to test this setup, the PLE spectra of an undoped GaAs wafer and a GaAs double heterostructure (DH) whose structure is shown in Fig. 6(a) was obtained for comparison at a photon flux of 1×10^{15} photons/s, which is shown in Fig. 6(b). The PL spectra of DH and GaAs at 400 nm excitation are shown in Fig. 6(c), where the photon flux on the GaAs sample was adjusted to get a sufficient signal at this excitation wavelength. The comparison of PL spectra shows a difference between peak positions which can be attributed to the different doping level of the two samples.[24] However, no significant difference in peak positions was observed at different excitation wavelengths for each sample. A GaAs wafer surface is known to have a very high (~10^7 cm/s) SRV.[25] Therefore, as the wavelength of the LED excitation is swept from deep red to UV, the PL signal decays sharply as carrier generation near the surface increases rapidly for shorter wavelengths.

In contrast, the passivation of both the front and back surfaces of a MBE grown GaAs layer in a DH significantly reduces the SRV and offers an improved SRH lifetime due to high quality MBE crystal growth. Hence, the PLE spectrum of a DH shows a significantly stronger and flatter PL signal compared to that of the GaAs wafer.

Furthermore, finer details in some portions in the PLE spectra can be obtained with a white LED, which still has a significantly larger photon flux in the red to blue region of spectrum compared to that of the halogen lamp.[13] The excitation wavelength can be adjusted by changing the grating angle of the monochromator as in a standard measurement using a halogen lamp. Figure 6(b) shows the PLE spectrum of a DH, obtained using a white LED. It has a signature indicated by an arrow near 700 nm, which can be attributed to the transitions from the spin orbit split valence band of GaAs.[26] If desired, the color LEDs can also be used to obtain a higher resolution in a small spectral region where

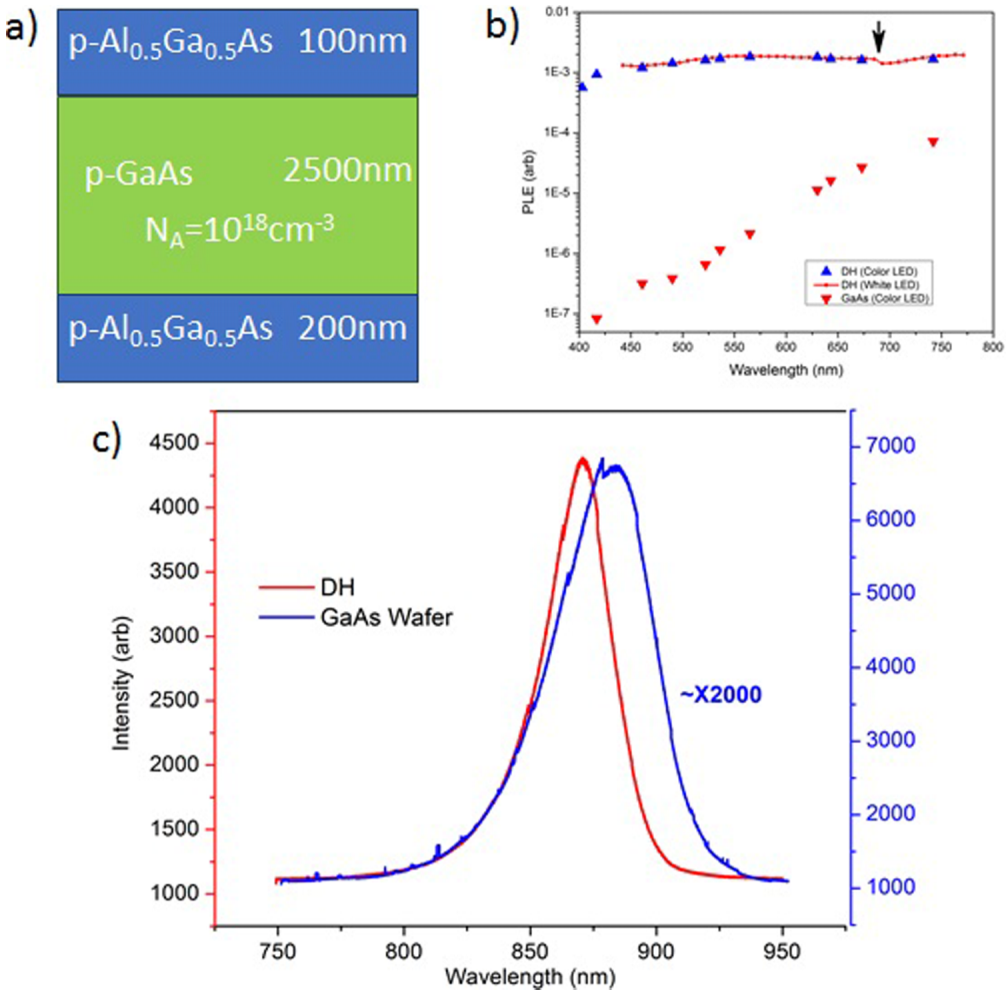

FIG. 6. (a) AlGaAs/GaAs double heterostructure schematic, adapted from Ref. 27; (b) comparison of PLE spectra of a GaAs double heterostructure (blue triangles and red dots) with that of a GaAs wafer (red upside-down triangles); and (c) the PL spectrum of a DH and a GaAs wafer.

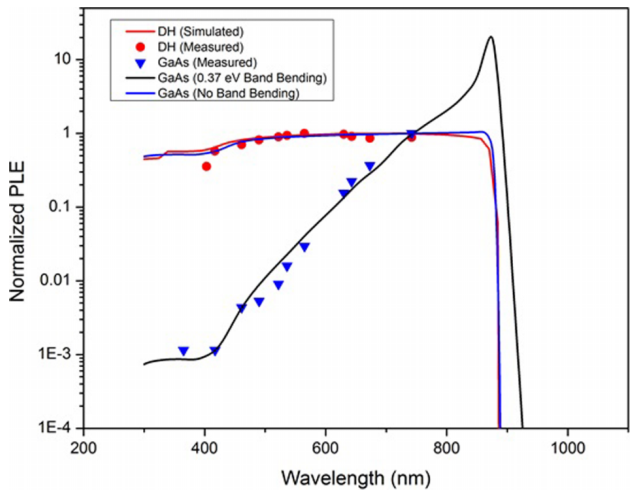

FIG. 7. PLE signal calculated analytically using Eq. (4). A reasonable qualitative comparison can be made with the experimental results in Fig. 6; overall, strong agreement is obtained.

higher incident flux is required, compared to that of the white LED.

At a preliminary level, the data obtained with this setup can be used to compare the SRV and SRH lifetime of different samples in a contactless manner. If one compares the measurements with two analytical curves calculated from Eq. (4) in Fig. 7, it is evident that a qualitative similarity between both the DH and bare GaAs wafer can be seen. These data suggest that the DH may experience a reduction in SRV of at least two orders of magnitude. For a more precise match, a detailed numerical model such as in Sentaurus is appropriate.[8] The Sentaurus model used to fit these data used the SRH lifetime and SRV as fitting parameters to match the data for the GaAs DH as reported in Ref. 8. For the GaAs wafer, the surface band bending was used as an additional parameter, which follows the description of trapped charge reported for an unpassivated GaAs surface in Ref. 28.

This information is valuable when a rough estimate of SRV is required as an indicator of surface quality in a multi-step material fabrication process. Because the exact emission is unknown for the measurements presented here, the plotted PLE is normalized to the value at the 742 nm wavelength for comparison with the simulation. Absolute PLE measurements would be necessary to yield the full value of the radiative recombination rate from emission at each wavelength. The absolute PLE measurement can be easily performed with an integrating sphere or compared to a reference cell with a known PLE response in order to determine SRV and SRH lifetime with improved accuracy when coupled with TRPL measurements and appropriate simulation framework.[8]

IV. CONCLUSIONS

We have introduced a low-cost PLE system and demonstrated its measurement capabilities using two GaAs samples. This instrument includes a novel approach of using LEDs as an illumination source, which provides higher intensity illumination than a halogen lamp, while being more cost efficient than a tunable laser. The use of monochromators at the entrance and exit of the system allows the reduction of IR broadband emission that might otherwise interfere with the measurements. As discussed in previous work,[8] with the application of numerical simulation this measurement technique coupled with TRPL should result in improved lifetime measurements.

ACKNOWLEDGMENTS

The authors thank Dr. Richard Ahrenkiel, Dr. Dean Levi, Dr. Steven W. Johnston, and Dr. Ana Kanevce of NREL, as well as Dr. Kyle Montgomery of UC Davis, for many helpful discussions and comments. Support was provided by the Department of Energy, under DOE Cooperative Agreement No. DE-EE0004946 ("PVMI Bay Area PV Consortium"), the National Renewable Energy Laboratory (NREL) as a part of the Non-Proprietary Partnering Program (NPO) under Contract No. DE-AC36-08-GO28308, as well as the Semiconductor Research Corporation, under Research Task No. 2110.003 ("Network for Photovoltaic Technologies").

APPENDIX: PLE LIGHT SOURCES

Some additional details of the sources used in our PLE setup are provided here. Colored and white-light LED spectra shown in Figs. 8 and 9, respectively, indicate that most of the spectrum relevant for mid-bandgap semiconductors such as GaAs is covered by the chosen system. Please note that the LED intensities do not necessarily correspond to experimental conditions exactly, since a constant photon flux condition was not enforced here. Furthermore, it was found that each LED has the majority of its spectrum within a full width at half maximum of 40 nm or less. This result allows us to treat each source as quasi-monochromatic, after taking the appropriate measures to eliminate leakage of long wavelengths from the source to detector.

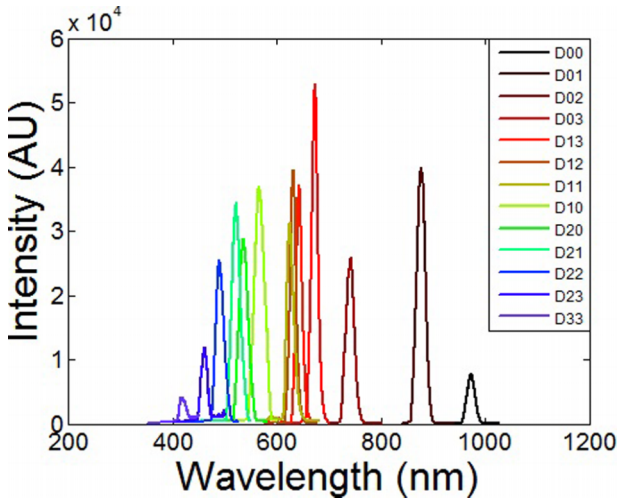

FIG. 8. Plot of LED spectra measured by PL through fiber optic aligned with the light beam at the position of the sample.

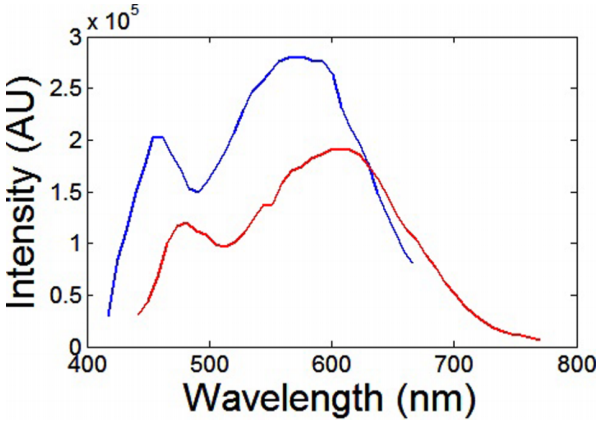

FIG. 9. Plot of spectra for white LEDs. Spectral coverage extends over the full visible spectrum plus some of the near-IR.

[1]J. S. Jie, W. J. Zhang, Y. Jiang, X. M. Meng, Y. Q. Li, and S. T. Lee, "Photoconductive characteristics of single-crystal CdS nanoribbons," Nano Lett. **6**(9), 1887–1892 (2006).

[2]Z. Zhang and J. T. Yates, Jr., "Direct observation of surface-mediated electron–hole pair recombination in TiO_2(110)," J. Phys. Chem. C **114**(7), 3098–3101 (2010).

[3]I. Favorskiy, D. Vu, E. Peytavit, S. Arscott, D. Paget, and A. C. H. Rowe, "Circularly polarized luminescence microscopy for the imaging of charge and spin diffusion in semiconductors," Rev. Sci. Instrum. **81**(10), 103902 (2010).

[4]G. D. Pettit, J. M. Woodall, and H. J. Hovel, "Photoluminescent characterization of GaAs solar cells," Appl. Phys. Lett. **35**(4), 335–337 (1979).

[5]G. S. Buller, J. S. Massa, and A. C. Walker, "All-solid-state microscope-based system for picosecond time-resolved photoluminescence measurements on II-VI semiconductors," Rev. Sci. Instrum. **63**(5), 2994–2998 (1992).

[6]G. Eda, H. Yamaguchi, D. Voiry, T. Fujita, M. Chen, and M. Chhowalla, "Photoluminescence from chemically exfoliated MoS_2," Nano Lett. **11**(12), 5111–5116 (2011).

[7]D. N. Hebert, J. A. N. T. Soares, and A. A. Rockett, "Photoluminescence and photoluminescence excitation spectroscopy of Cu(In,Ga)Se_2 thin films," MRS Proc. **1165**, 1165-M03–1165-M05 (2011).

[8]X. Wang, J. Bhosale, J. E. Moore, R. Kapadia, P. Bermel, A. Javey, and M. S. Lundstrom, "Photovoltaic material characterization with steady state and transient photoluminescence," IEEE J. Photovoltaics **5**(1), 282–287 (2015).

[9]O. D. Miller, E. Yablonovitch, and S. R. Kurtz, "Strong internal and external luminescence as solar cells approach the Shockley–Queisser limit," IEEE J. Photovoltaics **2**(3), 303–311 (2012).

[10]M. R. Khan, P. Bermel, and M. A. Alam, "Thermodynamic limits of solar cells with non-ideal optical response," in 39th Photovoltaic Specialists Conference, Tampa, FL, 16-19 June 2013.

[11]D. Berdebes, J. Bhosale, K. H. Montgomery, X. Wang, A. K. Ramdas, J. M. Woodall *et al.*, "Photoluminescence excitation spectroscopy for in-line optical characterization of crystalline solar cells," IEEE J. Photovoltaics **3**(4), 1342–1347 (2013).

[12]J. M. Woodall, G. D. Pettit, T. Chappell, and H. J. Hovel, "Photoluminescent properties of GaAs–GaAlAs, GaAs–oxide, and GaAs–ZnS heterojunctions," J. Vac. Sci. Technol. **16**(5), 1389–1393 (1979).

[13]J. S. Bhosale, "High signal-to-noise Fourier transform spectroscopy with light emitting diode sources," Rev. Sci. Instrum. **82**(9), 093103 (2011).

[14]S. Backus, C. G. Durfee III, M. M. Murnane, and H. C. Kapteyn, "High power ultrafast lasers," Rev. Sci. Instrum. **69**(3), 1207–1223 (1998).

[15]R. Haitz and J. Y. Tsao, "Solid-state lighting: 'The case'10 years after and future prospects," Phys. Status Solidi A **208**(1), 17–29 (2011).

[16]See http://www.roithner-laser.com for Roithner Laser Technik.

[17]M. C. Teich and B. E. A. Saleh, *Fundamentals of Photonics* (Wiley Interscience, Canada), p. 3.

[18]J. Bhosale, A. K. Ramdas, A. Burger, A. Muñoz, A. H. Romero, M. Cardona, R. Lauck, and R. K. Kremer, "Temperature dependence of band gaps in semiconductors: Electron-phonon interaction," Phys. Rev. B **86**(19), 195208 (2012).

[19]M. Sulkes and Z. Sulkes, "Measurement of luminescence decays: High performance at low cost," Am. J. Phys. **79**(11), 1104–1111 (2011).

[20]P. Wurfel, "The chemical potential of radiation," J. Phys. C: Solid State Phys. **15**(18), 3967 (1982).

[21]H. J. Schulz and M. Thiede, "Optical spectroscopy of $3d^7$ and $3d^8$ impurity configurations in a wide-gap semiconductor (ZnO: Co, Ni, Cu)," Phys. Rev. B **35**(1), 18 (1987).

[22]Schott North America, Inc., Short pass filters, 2015, http://www.us.schott.com/advanced_optics/english/products/filteroverviewdetail-shortpass.html.

[23]S. Chhajed, Y. Xi, Y. L. Li, T. Gessmann, and E. F. Schubert, "Influence of junction temperature on chromaticity and color-rendering properties of trichromatic white-light sources based on light-emitting diodes," J. Appl. Phys. **97**(5), 054506 (2005).

[24]G. Borghs, K. Bhattacharyya, K. Deneffe, P. Van Mieghem, and R. Mertens, "Band-gap narrowing in highly doped n- and p-type GaAs studied by photoluminescence spectroscopy," J. Appl. Phys. **66**(9), 4381–4386 (1989).

[25]L. Jastrzebski, J. Lagowski, and H. C. Gatos, "Application of scanning electron microscopy to determination of surface recombination velocity: GaAs," Appl. Phys. Lett. **27**, 537–539 (1975).

[26]B. Ketterer, M. Heiss, M. J. Livrozet, A. Rudolph, E. Reiger, and A. F. i Morral, "Determination of the band gap and the split-off band in wurtzite GaAs using Raman and photoluminescence excitation spectroscopy," Phys. Rev. B **83**(12), 125307 (2011).

[27]K. H. Montgomery, D. Berdebes, J. Bhosale, J. M. Woodall, and M. S. Lundstrom, "Photoluminescence excitation spectroscopy of p-GaAs surfaces and AlGaAs/GaAs interfaces supported by numerical modeling," in *2012 38th IEEE Photovoltaic Specialists Conference (PVSC)* (IEEE, 2012), pp. 000422–000426.

[28]E. Yablonovitch, B. J. Skromme, R. Bhat, J. P. Harbison, and T. J. Gmitter, "Band bending, Fermi level pinning, and surface fixed charge on chemically prepared GaAs surfaces," Appl. Phys. Lett. **54**(6), 555–557 (1989).